ANALYZING OCEANIC EDDY OFF SOUTHWESTERN TAIWAN

Yu-Hsin CHENG[a,*] and Chung-Ru HO[b]

[a] Department of Marine Environmental Informatics,
National Taiwan Ocean University, 2, Pei-Ning Rd., Keelung 20224, Taiwan;
Tel: +886(2)-2462-2192#6345; Fax. +886(2) -2462-0912
E-mail: 29981002@mail.ntou.edu.tw

[b] Department of Marine Environmental Informatics,
National Taiwan Ocean University, 2, Pei-Ning Rd., Keelung 20224, Taiwan;
Tel: +886(2)-2462-2192#6331; Fax. +886(2) -2462-0912
E-mail: b0211@mail.ntou.edu.tw

KEY WORDS: Remote Sensing, Oceanic Eddy, Southwestern Taiwan

Abstract: In this study, 19-year absolute dynamical topography data derived from multi-satellite altimetry were used to analyze the formation and the transformation of oceanic eddies in the sea off southwestern Taiwan. To track and detect eddies, we developed an integration filtering algorithm based on connected component labeling and the Okubo-Weiss parameter which can separate the flow field into deformation-dominated and vorticity-dominated regions. Area, relative vorticity, nonlinearity parameter, amplitude, central velocity, lifetime, propagation pathway and kinetic energy of eddies are determined by the integration filtering algorithm. The spatial and temporal characteristics of eddies are also revealed by the automatic eddy tracking method. The results indicate that the eddy is almost generated around 21.5ºN and 120ºE within a range of 100 km. However, the variation of the eddy may be affected by the migration of Kuroshio.

INTRODUCTION

The sea off southwestern Taiwan is a part of the northern South China Sea (SCS) where continental slop is northeast-southwest tilting. Some indicated eddies always move southwestward along the continental slope (Zhuang et al., 2010). The Luzon Strait, located between Taiwan and Luzon Islands, is an important channel for the water mass exchange between the western North Pacific and the SCS (Fig. 1). The Kuroshio intrusion forms an apparent anticyclonic loop current off southwestern Taiwan (Xue et al., 2004; Yuan et al., 2006) and is reproduced in numerical models (Chern et al., 2010; Sheu et al., 2010). The circulation in the SCS is strongly influenced by the volume transport pattern through the Luzon Strait (Hu et al., 2000). Many previous studies shown that the Kuroshio takes different intruding paths in the Luzon Strait (Caruso et al. 2006; Sheremet, 2001; Kuehl and Sheremet, 2009). Nan et al. (2011) demonstrated that the anticyclonic intrusion of the Kuroshio is a transient phenomenon and the paths could be classified into looping, leaking, and leaping path. The Kuroshio path in the Luzon Strait can change to different path in a few weeks.

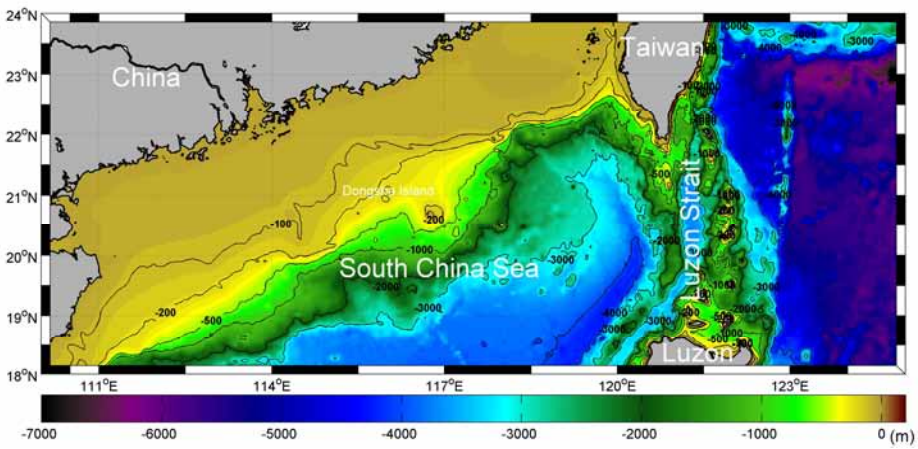

Figure 1: Topography map of northern SCS and Luzon Strait.

Mesoscale oceanic structures such as eddies are generally more energetic than the mean ocean kinetic energy and are one of important dynamical oceanography (Wyrtki et al., 1976; Richardson et al., 1983). In particular, they could exert a profound influence on the large-scale fluxes of momentum, heat, salt and even ocean-atmosphere system (Qiu and Chen, 2005; Jochum et al., 2008; Chow and Liu, 2012). The ocean eddies have long lived structures and aim to isolated rotating structure with compact forms (Robinson, 1983; Isern-Fontanet et al., 2006). Eddies could be identified well by altimetry data and from geostrophic velocity pattern (Chelton et al., 2011).

Previous studies have shown that there are anticyclonic eddies generated off northwestern Luzon Island and located at about 21°N, 117.5°E(Li et al. 1998; Yuan et al. 2007). Wang et al. (2008) used sea level anomaly (SLA) data and drifter data to analyze the temporal and spatial evolution of eddies in the northeastern SCS during winter, and found that the propagation speed of eddy is similar to the phase speed of Rossby waves in the northern SCS. Chen et al. (2011) reveals that there are more cyclonic eddies generated than anticyclonic eddy in the sea off southwestern Taiwan from October 1992 to October 2009. Although the process of eddies has been investigated by many studies, the conclusions are not consistent. To clarify the characteristics of the eddy, we investigate area, relative vorticity, nonlinearity parameter, central velocity, lifetime, propagation pathway and kinetic energy of the eddy base on an objective and threshold-free algorithm.

SATELLITE DATA

Maps of absolute dynamic topography (MADT) are applied to investigate the propagation of oceanic eddies in the sea off southwestern Taiwan from October 1992 to December 2011. The MADT data is provided by Archiving Validation and Interpretation of Satellite Data in Oceanography (AVISO), the Centre National d'Études Spatiales (CNES) of France. It is interpolated into a global grid with 1/4° resolution contain along-track sea surface heights derived from ERS, TOPEX/Poseidon, Jason, and Envisat altimeters. Absolute dynamic topography (ADT) is defined as the sea surface height above the geoid, thus it is obtained by summing sea level anomaly and mean dynamic topography which is derived using a multivariate objective analysis. This analysis is based on 4.5-year Gravity Recovery and Climate Experiment (GRACE), and 15-year altimetry and *in-situ* data (Argo floats and CTD).

METHODS

With the advance of science and technology, many different algorithm strive to identify eddies in satellite altimeter data or ocean model data. The first application of automated eddy detection using altimeter data is implemented based on the Okubo-Weiss parameter (Isern-Fontanet et al., 2003). Okubo (1970) and Weiss (1991) defined the Okubo-Weiss parameter (W) as

$$W = s_n^2 + s_s^2 - \zeta^2, \tag{1}$$

where s_n and s_s are the normal and shear strain, respectively, and the last term (ζ) is the relative vorticity of flow field. They are defined as

$$S_n = \frac{\partial v}{\partial x} + \frac{\partial u}{\partial y}, \quad S_s = \frac{\partial u}{\partial x} - \frac{\partial v}{\partial y}, \quad \zeta = \frac{\partial v}{\partial x} - \frac{\partial u}{\partial y}, \tag{2}$$

where u and v are the zonal and meridian components of velocity, respectively. Most previous studies (e.g., Sangrà et al., 2009) used the W-based method to define an eddy as connected regions where W parameter is below a specified negative threshold value. Using W parameter with a specified threshold value (W_T), Pasquero et al. (2001) separated the flow field into a vorticity-dominated region ($W < -W_T$), strain-dominated region ($W > W_T$) and background field ($|W| \le W_T$), where $W_T = 0.2\sigma_W$ with σ_W being the standard deviation in the study region. Several previous studies (Isern-Fontanet et al., 2006; Morrow et al., 2004) indicated that a threshold value is specified according to regional characteristics. However, how to specify the threshold value is very important and subjective. The Okubo-Weiss parameter is still significant in the physical meaning which implied a struggle between deformation field ($|s_n| + |s_s|$) and vorticity field ($|\zeta|$).

The eddy-detection algorithm in this study strives to achieve threshold-free identification of eddies using the ADT fields, and then we systematically study the characteristics of eddy in the SCS. This study assumed ocean is in

steady state, hence considered only the balance between pressure gradient and Coriolis force. The two-dimensional flow fields can be derived from MADT data through the geostrophic relations as

$$u = -\frac{g}{f}\frac{\partial \eta}{\partial y} = -\frac{g}{f}\frac{\partial \eta}{R_T \partial \phi}, v = \frac{g}{f}\frac{\partial \eta}{\partial x} = \frac{g}{f}\frac{\partial \eta}{R_T \cos\phi \partial \lambda}, \quad (3)$$

where g is gravitational acceleration, f is the Coriolis parameter, R_T is the mean earth radius (about 6371 km), ϕ, λ are latitude and longitude, and η is the absolute dynamic height. The integration filtering algorithm is developed based on connected component labeling and the Okubo-Weiss parameter. Four constraints are derived with the eddy characteristics described above. Eddy centers are determined with the following four constraints:

(1) vorticity-dominated region at the eddy center ($W < 0$);
(2) along a zonal direction, the row-component gradient of MADT must to reverse in sign across the eddy center;
(3) along a meridian direction, the column-component gradient of MADT must to reverse in sign across the eddy center; and
(4) MADT magnitude has a local extreme value at the eddy center.

Figure 2 the shows eddies detected by the algorithm from MADT data. Ocean eddies with different shape and vorticity sign could be detected well, confirming good consistency and accuracy of the eddy filter. The edge of eddies are delimitated by the outermost closed contour of MADT data.

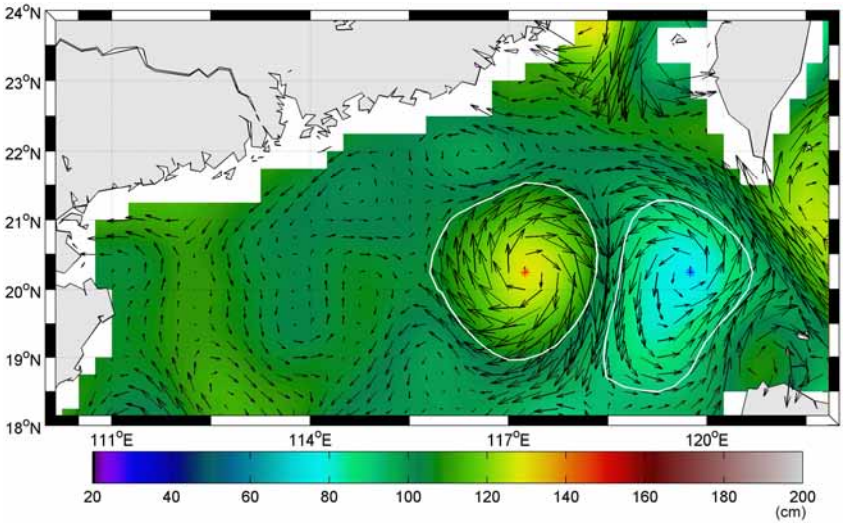

Figure 2: A map of MADT and eddy field detected on 10 Feb 2010. Velocity vectors are plotted per one grid point. Red and blue star are the centers of warm and cold eddy, respectively. The eddy edge is indicated by a white line.

RESULTS AND DISCUSSION

By the statistic of data from October 1992 to December 2011, the sea off southwestern Taiwan is a region with a high ratio of eddy generation (Fig. 3). The analogous results are also documented in some previous studies (Xiu et al., 2010; Cheng and Qi, 2010; Nan et al., 2011). We also obtained that there are more anticyclonic (warm) eddies (33) than cyclonic (cold) eddies (20) generated off southwestern Taiwan from 20.5°N to 22.5°N and from 119°E to 120.5°E. The Kuroshio intrusion is a significant influence not only on the general circulation of northern SCS but also eddy formation in northern SCS (Xiu et al., 2010).

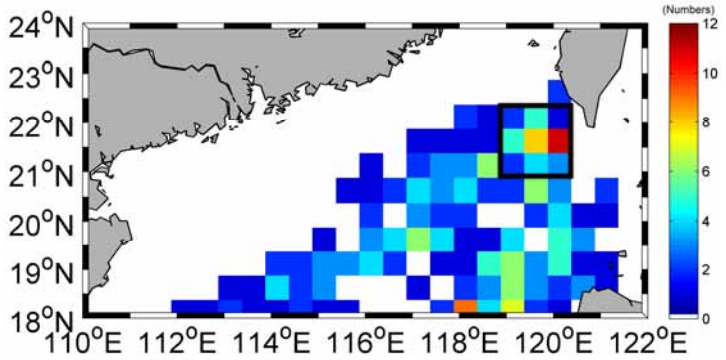

Figure 3: The numbers of eddy are generated at each pixel between 1993 and 2011. The black box denotes a high occurrence area of eddies.

In the SCS, most eddies propagate westward with speeds similar to the first-mode baroclinic Rossby wave (Bayler and Liu, 2008). Figure 4 shows the track of eddies generated off southwestern Taiwan. From the eddy tracking, we can know most anticyclonic eddies propagate southwestern ward along about 500 meter isobaths. Cyclonic eddies lingered relatively between 118°E and 121°E. Figure 5 is an example of eddy-evolution process using the automatic eddy tracking method. Furthermore, the kinematic properties of eddies are showed by statistical analysis (Table 1). Almost all properties of warm eddy are larger than cold eddy and move with very high advective nonlinearity parameter. The advective nonlinear eddy is defined as the ratio of eddy rotation speed (U) to eddy translation speed (C). The eddy is named nonlinear eddy when the ratio of U to C is larger than one (Fu et al., 2010; Chelton et al., 2011). However, the max area, eddy kinetic energy (EKE), and amplitude of warm eddy are larger than cold eddy.

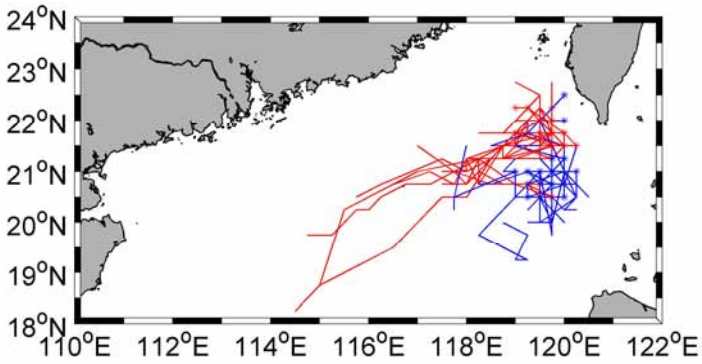

Figure 4: Tracking map of anticyclonic (warm) eddy and cyclonic (cold) eddy generated off southwestern Taiwan. Red and blue lines/stars denote pathways/centers of warm and cold eddy, respectively.

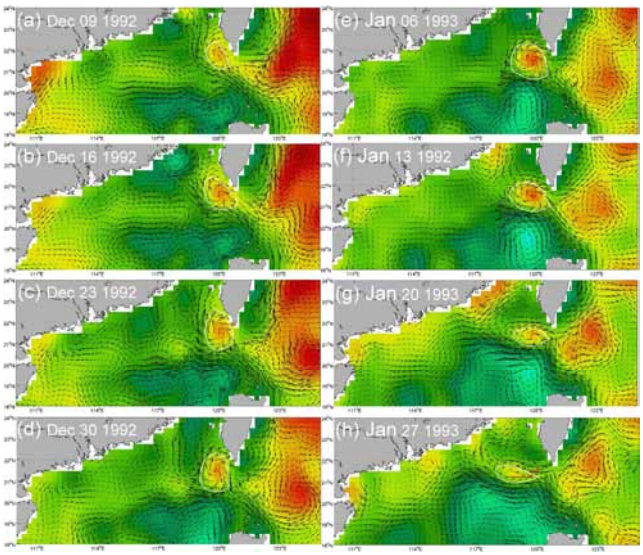

Figure 5: A map of MADT appear the evolutive process of warm eddy. Red lines, stars, and white cycle denote pathways, centers, and boundary, respectively.

Table 1: A summary of warm/cold eddy characteristics.

Property	Mean		Value Range		Standard Deviation	
	Warm Eddy	Cold Eddy	Warm Eddy	Cold Eddy	Warm Eddy	Cold Eddy
Area (km^2)	17984	17968	10000 ~ 31381	8281 ~ 28409	5377	5759
Relative Vorticity (10^{-6} rad/s)	-8.6	7.9	-12.9 ~ -4.9	6.0 ~ 13.2	2.0	1.7
Amplitude (cm)	10	8	4 ~ 20	4 ~ 10	3.5	1.7
Lifetime (weeks)	6.8	4.8	3 ~ 18	3 ~ 15	4.3	3.2
eddy kinetic energy (cm^2/s^2)	482	334	114 ~ 1321	194 ~ 626	254	103
Translation speed (m/s)	0.08	0.07	0.05 ~ 0.11	0.02 ~ 0.12	0.02	0.02
Advective nonlinearity parameter	inf	inf	7 ~ inf	4 ~ inf	-	-

CONCLUSIONS

Nineteen years of absolute dynamical topography (ADT) maps are analyzed to investigate ocean-eddy formation and propagation in the sea off southwestern Taiwan. Eddy trajectories are also obtained by the automated-tracking integration filtering algorithm based on connected component labeling and the Okubo-Weiss parameter. The results show Ocean eddies with different shape and vorticity sign could be detected very well. According to the analyses of ADT data from 1992 to July 2011, the results indicate that quantities of eddies are generated in a region from 20.5°N to 22.5°N and from 119°E to 120.5°E. Most anticyclonic eddies propagate southwestern ward and cyclonic eddies lingered relatively between 118°E and 121°E. The relative vorticity, amplitude, lifetime, and EKE of warm eddies could be larger than cold eddies. On the other hand, not only anticyclonic eddy are translation with very high advective nonlinearity parameter but also cyclonic eddy in the SCS. Nevertheless, this study just performs the statistical analysis and automatic tracking. More detail researches are necessary to understand the dynamic process and generative mechanism of eddies.

REFERENCES:

Bayler, E. J., and Z. Liu, 2008. Basin-scale wind-forced dynamics of the seasonal southern South China Sea gyre. J. Geophys. Res., 113, C07014, doi:10.1029/2007JC004519.

Caruso, M. J., G. G. Gawarkiewicz, and R. C. Beardsley, 2006. Interannual variability of the Kuroshio intrusion in the South China Sea. J. Oceanogr., 62, 559–575, doi:10.1007/s10872-006-0076-0.

Chelton, D. B., M. G. Schlax, and R. M. Samelson, 2011. Global observations of nonlinear mesoscale eddies. Prog. Oceanogr., 91, 167−216.

Chen, G. X., Y. J. Hou, and X. Q. Chu, 2011. Mesoscale eddies in the South China Sea: Mean properties, spatio-temporal variability and impact on thermohaline structure. J. Geophys. Res., 116, C06018, doi:10.1029/2010JC006716.

Cheng, X. H., and Y. Q. Qi, 2010. Variations of eddy kinetic energy in the South China Sea. J. Oceanogr., 66, 85−94, doi:10.1007/s10872-010-0007-y.

Chern, C.-S., S. Jan, and J. Wang, 2010. Numerical study of mean flow patterns in the South China Sea and the Luzon Strait. Ocean Dyn., 60, 1047–1059, doi:10.1007/s10236-010-0305-3.

Fu, L.-L., D. B. Chelton, P.-Y. Le Traon, and R. Morrow, 2010. Eddy dynamics from satellite altimetry. Oceanogr., 23, 14-25, doi:10.5670/oceanog.2010.02.

Hoe, C., and Q. Liu, 2012. Eddy effects on sea surface temperature and sea surface wind in the continental slope region of the northern South China Sea. Geophys. Res. Lett., vol. 39, L02601, 5 PP., 2012 doi:10.1029/2011GL050230

Hu, J., H. Kawamura, H. Hong, and Y. Qi, 2000. A review on the currents in the South China Sea: Seasonal circulation, South China Sea warm current and Kuroshio intrusion. J. Oceanogr., 56, 607–624, doi:10.1023/A:1011117531252.

Isern-Fontanet, J., E. Garcia-Ladona, and J. Font, 2006. Vortices of the Mediterranean Sea: An altimetric perspective, J. Phys. Oceanogr., 36, 87-103.

Isern-Fontanet, J., Garcia-Ladona, E., Font, J., 2003. Identification of marine eddies from altimetric maps. J. Atmos.

Oceanic Technol. 20, 772−778.

Jochum, M., Danabasoglu, G., Holland, M., Kwon, Y.O., Large, W.G., 2008. Ocean viscosity and climate. J. Geophys. Res., 113, C06017.

Kuehl, J. J., and V. A. Sheremet, 2009. Identification of a cusp catastrophe in a gap-leaping western boundary current. J. Mar. Res., 67, 25–42, doi:10.1357/002224009788597908.

Li, L., W. D. Nowlin Jr., and J. L. Su, 1998. Anticyclonic rings from the Kuroshio in the South China Sea. Deep Sea Res., Part I, 45, 1469−1482, doi:10.1016/S0967-0637(98)00026-0.

Morrow, R., F. Birol, D. Griffin, and J. Sudre, 2004. Divergent pathways of cyclonic and anti-cyclonic ocean eddies. Geophys. Res. Lett., 31, L24311, doi:10.1029/ 2004GL020974.

Nan, F., H. Xue, F. Chai, L. Shi, M. Shi, and P. Guo, 2011. Identification of different types of Kuroshio intrusion into the South China Sea. Ocean Dyn., 61, 1291–1304, doi:10.1007/s10236-011-0426-3.

Nan, F., H. Xue, P. Xiu, F. Chai, M. Shi, and P. Guo. 2011. Oceanic eddy formation and propagation southwest of Taiwan, J. Geophys. Res., vol. 116, C12045, 15 PP., 2011 doi:10.1029/2011JC007386

Okubo, A., 1970. Horizontal dispersion of floatable particles in the vicinity of velocity singularities such as convergences. Deep-Sea Res., 17, 445-454.

Pasquero, C., A. Provenzale, and A. Babiano, 2001. Parametrization of dispersion in two-dimensional turbulence. J. Fluid Mech., 439, 279-303.

Qiu, B., and S. Chen, 2005. Eddy induced heat transport in the subtropical North Pacific from Argo, TMI and altimetry measurements. J. Phys. Oceanogr., 35, 458−473, doi:10.1175/JPO2696.1.

Richardson, P. L., 1983. Eddy kinetic energy in the North Atlantic Ocean from surface drifters, J. Geophys. Res., 88, 4355-4367.

Robinson, A. R., 1983. Eddies in Marine Science; Robinson, A. R., Ed., Springer, New York, pp. 609.

Sangrà, P., A. Pascual, A. Rodríguez-Santana, F. Machín, E. Mason, J. C. McWilliams, J. L. Pelegrí, C. Dong, A. Rubio, J. Arístegui, Á. Marrero-Díaz, A. Hernández-Guerra, A. Martínez-Marrero, and M. Auladell, 2009. The Canary Eddy Corridor: A major pathway for long-lived eddies in the subtropical North Atlantic. Deep-Sea Res. I, 56, 2100-2114.

Sheremet, V. A., 2001. Hysteresis of a western boundary current leaping across a gap. J. Phys. Oceanogr., 31, 1247–1259, doi:10.1175/1520-0485(2001)031<1247:HOAWBC>2.0.CO;2.

Sheu, W.-J., C.-R. Wu, and L.-Y. Oey, 2010. Blocking and westward passage of eddies in the Luzon Strait. Deep Sea Res., Part II, 57, 1783–1791, doi:10.1016/j.dsr2.2010.04.004.

Wang, D., H. Xu, J. Lin, and J. Hu, 2008. Anticyclonic eddies in the northeastern South China Sea during winter 2003/2004. J. Oceanogr., 64, 925−935, doi:10.1007/s10872-008-0076-3.

Weiss, J., 1991. The dynamics of enstrophy transfer in two dimensional hydrodynamics. Physica. D., 48, 273-294.

Wyrtki, K., L. Magaard, and J. Hager, 1976. Eddy energy in the oceans. J. Geophys. Res., 81, 2641-2646.

Xiu, P., F. Chai, L. Shi, H. J. Xue, and Y. Chao, 2010. A census of eddy activities in the South China Sea during 1993-2007. J. Geophys. Res., 115, C03012, doi:10.1029/2009JC005657.

Xue, H., F. Chai, N. Pettigrew, D. Xu, M. Shi, and J. Xu, 2004. Kuroshio intrusion and the circulation in the South China Sea. J. Geophys. Res., 109, C02017, doi:10.1029/2002JC001724.

Yuan, D., W. Han, and D. Hu, 2006. Surface Kuroshio path in the Luzon Strait area derived from satellite remote sensing data. J. Geophys. Res., 111, C11007, doi:10.1029/2005JC003412.

Yuan, D., W. Han, and D. Hu, 2007. Anticyclonic eddies northwest of Luzon in summer−fall observed by satellite altimeters. Geophys. Res. Lett., 34, L13610, doi:10.1029/2007GL029401.

Zhuang, W., Y. Du, D. Wand, Q. Xie, and S. Xie, 2010. Pathways of mesoscale variability in the South China Sea. Chin. J. Oceanol. Limnol., 28, 1055–1067, doi:10.1007/s00343-010-0035-x.